



CHORUS

This is the accepted manuscript made available via CHORUS. The article has been published as:

Time evolution of electron structure in femtosecond heated warm dense molybdenum

F. Dorchies, V. Recoules, J. Bouchet, C. Fourment, P. M. Leguay, B. I. Cho, K. Engelhorn, M. Nakatsutsumi, C. Ozkan, T. Tschentscher, M. Harmand, S. Toleikis, M. Störmer, E. Galtier, H. J. Lee, B. Nagler, P. A. Heimann, and J. Gaudin

Phys. Rev. B **92**, 144201 — Published 21 October 2015

DOI: [10.1103/PhysRevB.92.144201](https://doi.org/10.1103/PhysRevB.92.144201)

Time evolution of electron structure in femtosecond heated warm dense molybdenum

F. Dorchies,^{1,*} V. Recoules,² J. Bouchet,² C. Fourment,¹ P.M. Leguay,¹ B.I. Cho,³ K. Engelhorn,⁴ M. Nakatsutsumi,⁵ C. Ozkan,⁵ T. Tschentscher,⁵ M. Harmand,⁶ S. Toleikis,⁶ M. Störmer,⁷ E. Galtier,⁸ H.J. Lee,⁸ B. Nagler,⁸ P.A. Heimann,⁸ and J. Gaudin¹

¹Univ. Bordeaux, CNRS, CEA, CELIA (Centre Lasers Intenses et Applications), UMR 5107, F-33400 Talence, France

²CEA-DAM-DIF, F-91297 Arpajon, France

³Department of Physics and Photon Science, Gwangju Institute of Science and Technology (GIST), Gwangju, Korea

⁴Lawrence Berkeley National Laboratory, Berkeley, USA

⁵European XFEL, Hamburg, Germany

⁶DESY, Hamburg, Germany

⁷Helmholtz Zentrum Geesthacht, Geesthacht, Germany

⁸SLAC National Accelerator Laboratory, Menlo Park, USA

The time evolution of the electron structure is investigated in a molybdenum foil heated up to the warm dense matter regime by a femtosecond laser pulse, through time-resolved XANES spectroscopy. Spectra are measured with independent characterization of temperature and density. They are successfully compared with *ab initio* quantum molecular dynamic calculations. We demonstrate that the observed white line in the L3-edge reveals the time evolution of the electron density of state from the solid to the hot (a few eV) and expanding liquid. The data indicate a highly non-equilibrated state, 5 ps after heating.

PACS numbers: 52.50.Jm, 61.05.cj, 71.22.+i, 78.47.J-

The study of Warm Dense Matter (WDM) shows a strong renewed interest, due to advances in transient techniques to create matter in this regime¹⁻⁶, and in first principles calculations to simulate the physical properties^{7,8} involved in various physical domains such as planetary physics⁹, inertial confinement fusion¹⁰, and applied laser processes¹¹. The difficulty of modeling comes from the atomic level: disordered matter, partially degenerate electrons and strongly coupled ions. In most situations, *ab initio* Quantum Molecular Dynamic (QMD) simulations are required, considering both the ion spatial distribution through molecular dynamics and the near-continuum electron structure through Density Functional Theory (DFT). DFT is the cornerstone of calculations of most physical properties (equations of state, transport coefficients, ...). Valuable experimental data are needed to support the constant improvements of numerical codes¹².

In principle, X-ray Absorption Near-Edge Spectroscopy (XANES) provides access to the electronic structure, since it probes near-continuum unoccupied states from core levels. Alternatively, X-ray Emission Spectroscopy (XES) has been proposed to probe the corresponding occupied states¹³. Yet little data are available. The first were obtained near the K-edge of warm dense aluminum. At solid density and above, the near free electron gas Density Of State (DOS) was essentially unchanged. The main modifications observed in the XANES spectra concerned the K-edge shift associated with the change in the core-level screening¹⁴. During expansion below the solid density, in contrast, the electron DOS was progressively modified during the metal - non-metal transition, and was revealed by a pre-edge peak in XANES spectra^{15,16}. In another study, the metallization of warm dense silica at high temperature has been

diagnosed by the Si K-edge shift from the bottom of the valence band (insulator) down to the Fermi energy (semi-metal)¹⁷. Time-resolved XANES (Tr-XANES) measurements have also been reported on warm dense copper (noble metal). They were used to retrieve the temporal evolution of the electronic temperature through comparison to theoretical calculations¹⁸, and to address the electron - ion equilibration dynamics in rapidly heated matter.

In this letter, we present Tr-XANES study of femtosecond laser-heated molybdenum. This last has been chosen as a prototype transition metal. Their near-continuum electron structure is dominated by a *d*-band that plays a key role in their physical properties. The white line observed in the L3-edge spectra is used to reveal the rapid time evolution of the electron DOS. Spectra are measured with independent control of temperature and density, and they are successively compared with *ab initio* QMD calculations. The experimental data suggest a non-equilibrium state in the first picoseconds, where the DOS is still solid-state-like while the electron temperature reaches several eV.

The principle of the XANES measurement is presented in Fig. 1a. Spectral features near the Mo L3-edge are dominated by photoabsorption that couples the $2p_{3/2}$ core level with vacant $4d$ -states above the Fermi energy E_F . As the $4d$ -band is highly localized in energy, a strong absorption peak also called the White Line (WL) is expected. This WL is conventionally interpreted as resulting from the unoccupied electron DOS in condensed matter¹⁹. We further demonstrate that the WL directly reveals the electron DOS spectral shape, in a large thermodynamical domain from solid to WDM.

The experiment has been performed at the Matter in Extreme Conditions (MEC) instrument at the Linac

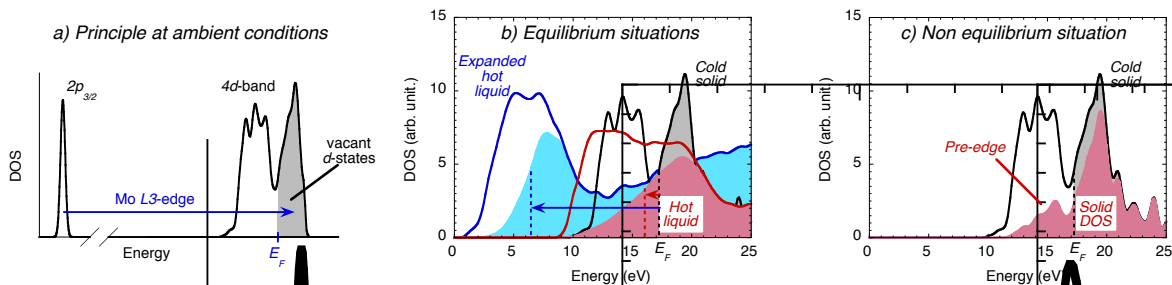


FIG. 1: (color online). (Left *a*) Principle of L3-edge XANES as a probe of the Mo 4*d*-band. (Center *b*) Electronic Density of State (DOS) from QMD calculations, for three representative situations (full lines): (*Cold solid*) $\rho = 10.12$ g/cc, $T_e = T_i = 300$ K; (*Hot liquid*) $\rho = 9.56$ g/cc, $T_e = T_i = 20,000$ K; (*Expanded hot liquid*) $\rho = 5$ g/cc, $T_e = T_i = 10,000$ K. The respective unoccupied states responsible for the observed Mo L3-edge white line, are indicated with filled areas drawn below the full DOS. (*Dotted lines*) Corresponding Fermi energies. (Right *c*) Total and unoccupied DOS when considering the non equilibrium situation: $\rho = 10.12$ g/cc (solid), $T_i = 300$ K (cold lattice) and $T_e = 20,000$ K (hot electrons).

Coherent Light Source (LCLS). The experimental setup and the XANES measurement procedure have been previously described²⁰. A 100 nm thick Mo sample deposited on a 100 μ m thick plastic substrate, and covered by an 8 nm layer of amorphous carbon, is heated by a femtosecond laser pulse (300 fs, 4 J/cm², *p*-polarized at 800 nm) at 12° incidence angle. It is probed at different delays by the ultrashort x-ray pulse delivered by the LCLS. The synchronization has been monitored during the experiment, by using the plasma switch method²¹, providing ≤ 1 ps temporal jitter. For each delay, about 20 successive shots are accumulated in order to obtain a XANES spectrum with a few % noise level.

The thermodynamic conditions of the sample have been determined by using the 1D Lagrangian code ESTHER²². The laser absorption is calculated by solving the Helmholtz equations. The time evolution is described by hydrodynamics coupled to a two-temperature (electron and ion) multiphase equation of state²³, with consistent ion heat capacity. The electron-ion energy transfer is described by the electron-phonon coupling factor taken from Lin et al.²⁴. The thermal equilibrium is reached in 2 ps. In the first picoseconds, the Mo layer density remains close to that of the solid. After ~ 20 ps, because of the high induced pressure, the sample significantly expands, leading to the simultaneous decrease of both temperature and density. At long delays, a portion of the sample expands (laser side), while the other part is slightly constrained by the plastic substrate.

In order to constrain the hydrodynamic simulations, an independent experiment has been performed on the Eclipse laser facility at the CELIA laboratory, using the same samples and similar laser parameters with a fluence varied from 2 to 10 J/cm². Fourier Domain Interferometry has been used as a standard technique to determine the surface velocity²⁵. A good agreement is found ($\leq 20\%$) with hydrodynamic simulations. Densities and temperatures corresponding to the delays of XANES measurements are reported in Fig. 2. Data are averaged along the Mo layer thickness and the inhomoge-

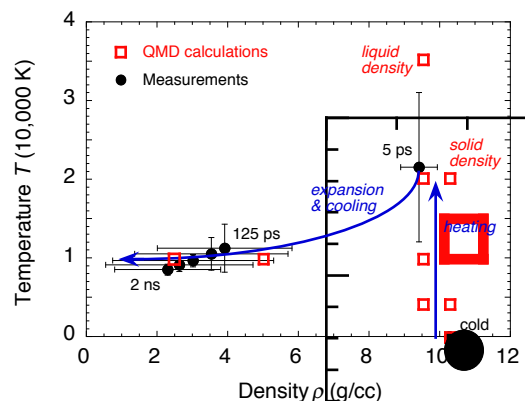


FIG. 2: (color online). Summary of warm dense Mo density and temperature conditions studied in this paper.

geneities are reported in the error bars (standard deviations). At short delay (several ps), we probe near solid density at $21,500 \pm 9,500$ K. At longer delays (up to 2 ns), the sample is still hot ($\sim 10,000$ K), but the density drops to a few g/cc. The conditions considered for QMD simulations, representative of the experiment are also reported in Fig. 2.

Some characteristic Mo L3-edge XANES spectra are reported in Fig. 3. They are dominated by a white line with a ~ 5 eV width. Its amplitude and spectral shift are plotted in Fig. 4 as a function of the delay. In the first picoseconds after heating, the WL amplitude is decreased to $85 \pm 5\%$, then increases slightly to reach $\sim 90\%$ of the cold value at longer delays (~ 1 ns). The evolution of the spectral shift is not as fast. It takes a few 100 ps to reach a maximal value of -1.10 ± 0.15 eV. The time scales of the temperature and density evolution (cf. Fig. 2) suggest that the WL amplitude decrease could be associated to the fast temperature increase, while the WL negative spectral shift could result from the slower density decrease. Among all the experimental data, the spectrum registered at 5 ps is the only one to present

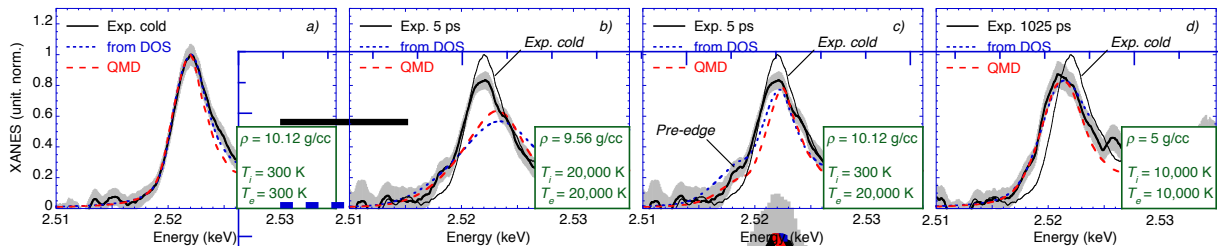


FIG. 3: (color line). Some representative XANES spectra measured before the laser heating (cold: *a*)), just after heating when the sample is supposed to be hot and still near solid density (5 ps time delay: *b*) and *c*) and at longer time during hydrodynamic expansion that reduces both the temperature and density (1025 ps time delay: *d*). Measurements (full lines) are compared with simple calculations from the electron DOS (dotted lines), and with full QMD calculations (dashed lines). The measurement uncertainty is illustrated by the grey area. The spectrum observed for the cold sample is reported as a reference (thin line). The values of density and temperature used for the calculations are indicated in the respective plots. The calculation considers equilibrated temperatures in *a*), *b*) and *d*), and a non-equilibrium situation in *c*).

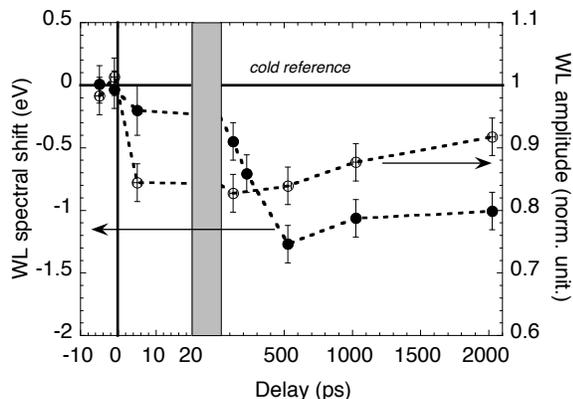


FIG. 4: Evolution of the Mo L3-edge White Line (WL) as a function of time delay after heating. The delay scale (x -axis) has been broken in order to highlight the different temporal behaviors of both the amplitude (decrease of $\sim 15\%$ in the first picoseconds) and the negative spectral shift (more gradual and occurring over a few 100 ps). The spectral shift is defined by the half-height position of the WL rising edge.

a pre-edge structure, just before the WL. Note that it significantly emerges from the cold WL outside the experimental uncertainty²⁰.

To simulate molybdenum at a given thermodynamic state, we perform molecular dynamics simulations using the *ab initio* plane wave density functional theory (DFT) code ABINIT^{26,27}. DFT is applied together with Generalized Gradient Approximation²⁸. Simulations are performed in the framework of the projected augmented wave (PAW) method^{29,30} using a PAW data set including semi-core states which has been benchmarked extensively against physical properties obtained from experiments³¹. The PAW data set is generated with 14 outer electrons ($4s^2 4p^6 4d^5 5s^1$).

To reproduce the Mo L3-edge white line, a first approach consists in performing an *ab initio* calculation of the absorption cross section following the methodology

described in³² (more details are given in the Supplementary Materials). A second analytical approach is considered, based on the simple picture presented in Fig. 1*a*. The electron d -DOS obtained from *ab initio* calculations is multiplied by $(1 - f(E))$, where E is the energy and $f(E)$ the Fermi-Dirac occupation factor depending on the electronic temperature T_e . The resulting unoccupied DOS is then convoluted by a Lorentzian function that reflects the $2p_{3/2}$ core-hole lifetime. Its width is 1.56 eV FWHM, as obtained from an atomic configuration-average calculation³³. The two calculated spectra are compared to the experiment in Fig. 3*a*), considering the case of cold solid Mo. A very good agreement is obtained, validating the WL as a direct diagnostic of the $4d$ -band DOS.

The electron DOS has been calculated by QMD for all conditions reported in Fig. 2. Some representative results are plotted in Fig. 1*b*. The cold solid exhibits a structured $4d$ -band, mainly composed of two separate energy regions. The first one is filled up to the Fermi energy (occupied states). The second one is empty (unoccupied states resulting in the WL). The Fermi level is located in the deep minimum which is a characteristic feature of bcc transition metals. The $4d$ -band envelop is significantly affected when the temperature increases. The structures disappear to form a fairly flat and slightly broadened band, as illustrated in the calculation performed at 20,000 K. Such behavior is observed at temperatures as low as 4,000 K confirming that it is highly correlated with the transition from solid to liquid phase, as previously reported in photoelectron spectroscopy measurements^{34,35}. The decrease in density results in a negative energy shift of both the $4d$ -band and the Fermi energy E_F . The shift of E_F is -1.0 eV when going from solid (10.12 g/cc) down to liquid density (9.56 g/cc), then the shift reaches -10.5 and -15.8 eV at 5 and 2.5 g/cc.

These electronic DOS changes result in a modification of the XANES spectra. Both calculations (WL estimated

from the DOS and QMD full XANES simulations) are compared with experimental data in Fig. 3. The DOS blurring and broadening occurring at high temperature result in a decrease of the WL amplitude. The level of this decrease fits well with the observations at relatively long delays (≥ 100 ps when the temperature is close to 10,000 K). The agreement is less satisfactory at the shortest delay (5 ps), which will be discussed.

The DOS energy shift with the density results in a WL energy shift. But, a proper calculation requires additional information about the core-level energy ($2p_{3/2}$) that is also modified with the density, since the atomic potential screening is affected. The core-level shift cannot be directly calculated by the QMD simulations, in which only the 14 outer electrons are explicitly treated. Therefore, a calculation has been performed using the DFT Wien2k code, taking explicitly into account all the electrons in the Mo electronic cloud³⁶ (see Supplementary Materials for more detail). Both the $2p_{3/2}$ energy level and E_F are predicted to \sim linearly decrease when the density decreases from the solid to a few g/cc, before converging towards the isolated atom values (below 1 g/cc). Consequently, the E_F decrease is mainly compensated by the core-level shift. From the solid down to the liquid density, this results in a quasi unmodified energy position for the WL, in agreement with the measurements at the shortest delays. At 5 and 2.5 g/cc, residual WL energy shifts of ~ -0.9 and ~ -1.8 eV are predicted by the calculations, in close agreement with the spectra measured at the longest delays (cf. Fig. 3d).

The L3-edge Mo XANES spectra are well reproduced by both calculation approaches, (except the measurement at 5 ps). This agreement confirms that the observed WL modifications can be interpreted in the whole density-temperature domain explored in this study, in terms of associated DOS changes: *i*) the WL amplitude decrease reveals the DOS blurring when the temperature increases, *ii*) the WL negative shift is due to the DOS energy shift when the density decreases.

The spectrum registered at the shortest delay (5 ps) exhibits a pre-edge structure. In Fig. 3b, we report calculations performed at 20,000 K and liquid density (expected average conditions at 5 ps, cf. Fig. 2). They show a WL amplitude decrease significantly stronger than observed, as well as a broad slope in the rising edge due to the temperature dependence of $f(E)$. This is clearly different from the pre-edge observed in the experiment. The XANES spectrum measurement could be affected by the large temperature gradient as a function of depth expected at short delays. By considering a deliberately extreme situation (half of the Mo layer at 300 K, and the other half at 35,000 K), the average XANES spectrum remains similar to the one calculated at 20,000 K, and does not result in a pre-edge. A satisfactory agreement is found, if we consider a non-equilibrium situation where the electronic temperature is $T_e = 20,000$ K, while the DOS is still structured as in the cold solid (cf. Fig. 3c). The corresponding unoccupied DOS is plotted in Fig. 1c.

The increase in T_e promotes some electrons from the first energy region (initially full) to the second one (initially empty). That results in a peak pattern in the unoccupied DOS just below E_F , responsible for the pre-edge structure observed in the XANES spectrum. A similar feature has been observed in previous calculations, when increasing the ionization state of bcc Mo³⁷.

Such a non-equilibrium situation is unexpected as late as 5 ps after heating. The electron DOS is supposed to adapt very rapidly to the atomic spatial distribution (on a femtosecond time scale). If we consider that the sample transforms into a hot liquid as soon as the ionic temperature exceeds the melting temperature, then the time scale should be even shorter than the electron-ion thermal equilibration estimated to be achieved in 2 ps²⁴. Recent papers suggest that the electron-ion coupling could be reduced in the WDM regime, which would lead to longer equilibration times^{38,39}. Previous studies suggested that a hot electron population (a few eVs) could strengthen the lattice stability and thus delay the melting time^{40,41}. This is expected for some noble metals, but not for transition metals such as molybdenum⁴². A final possibility is that additional delay is needed for the atomic spatial distribution to change after the melting temperature is reached, or because of hydrodynamic effects.

In summary, we present time-resolved XANES spectra measured near the L3-edge of a molybdenum foil rapidly heated by a femtosecond laser pulse. The hydrodynamic expansion has been carefully estimated from calculations and optical measurements. Just after heating, the warm dense molybdenum temperature reaches a few eV at near solid density. Then, the density progressively decreases down to a few g/cc. XANES spectra are dominated by a white line whose shape and time evolution are successively reproduced by *ab initio* QMD calculations. We demonstrate that it can be directly interpreted in terms of the unoccupied electron DOS near the continuum. From this study, we deduce that the electron DOS is blurred and broadened when the temperature increases beyond melting. When the density decreases, the DOS shifts towards low energies. In the XANES spectra, this last effect is partially compensated by the $2p_{3/2}$ core-level energy shift due to the change in screening. At the shortest time delay (5 ps), the observed XANES spectrum suggests a non-equilibrium situation (a high electron temperature ~ 2 eV, but still solid-state-like electron DOS). Further experimental studies are needed to find out the details of such a non equilibrium persistence during the ultrafast transition from solid to WDM.

This work was supported by the French Agence Nationale de la Recherche, under grant OEDYP (ANR-09-BLAN-0206-01) and by the GENCI program providing computational time under the program GEN6046 and GEN6454. The authors gratefully acknowledge Benoit Chimier and Olivier Peyrusse for fruitful discussions respectively concerning hydrodynamic simulations and XANES spectra calculations, Rodrigue Bouilaud and Laurent Merzeau for their technical assis-

tance, and Frédéric Burgy and Fanny Froustey for laser operation at CELIA. The authors thanks Marc Torrent for his great help with ABINIT simulations. B.I. Cho acknowledges support from the National Research Foundation of Korea (NRF-2013R1A1A1007084, NRF-2015R1A5A1009962) and the TBP research project of GIST. Portions of this research were carried out at the

Linac Coherent Light Source (LCLS) at the SLAC National Accelerator Laboratory. LCLS is an Office of Science User Facility operated for the US Department of Energy Office of Science by Stanford University. The MEC instrument has additional support from the DOE Office of Science, Office of Fusion Energy Sciences under contract No. SF00515.

-
- * Electronic address: dorchies@celia.u-bordeaux1.fr
- ¹ M. Koenig *et al.*, Phys. Rev. Lett. **74**, 2260 (1995).
 - ² G.W. Collins *et al.*, Science **281**, 1178 (1998).
 - ³ M. Knudson *et al.*, Phys. Rev. Lett. **87**, 225501 (2001).
 - ⁴ P.K. Patel *et al.*, Phys. Rev. Lett. **91**, 125004 (2003).
 - ⁵ K. Widmann *et al.*, Phys. Rev. Lett. **92**, 125002 (2004).
 - ⁶ A. Lévy *et al.*, Phys. Plasmas **22**, 030703 (2015).
 - ⁷ D. Hohl *et al.*, Phys. Rev. Lett. **71**, 541 (1993).
 - ⁸ S. Mazevet and G. Zérah, Phys. Rev. Lett. **101**, 155001 (2008).
 - ⁹ T. Guillot, Science **286**, 72 (1999).
 - ¹⁰ J. Lindl, Phys. Plasmas **2**, 3933 (1995).
 - ¹¹ J. Chan *et al.*, Opt. Lett. **26**, 1726 (2001).
 - ¹² National Research Council, *Frontiers in High Energy Density Physics: The X-Games of Contemporary Science* (National Academic Press, Washington, D.C., 2003).
 - ¹³ S.M. Vinko *et al.*, Phys. Rev. Lett. **104**, 225001 (2010).
 - ¹⁴ A. Benuzzi-Mounaix *et al.*, Phys. Rev. Lett. **107**, 165006 (2011).
 - ¹⁵ F. Dorchies *et al.*, Phys. Rev. Lett. **107**, 245006 (2011).
 - ¹⁶ A. Lévy *et al.*, Phys. Rev. Lett. **108**, 055002 (2012).
 - ¹⁷ A. Denoëud *et al.*, Phys. Rev. Lett. **113**, 116404 (2014).
 - ¹⁸ B.I. Cho *et al.*, Phys. Rev. Lett. **106**, 167601 (2011).
 - ¹⁹ *X-ray absorption: principles, applications, techniques of EXAFS, SEXAFS and XANES*, D. C. Koningsberger and R. Prins, Ed. J. Wiley & Sons, New York 1988.
 - ²⁰ J. Gaudin *et al.*, Scientific Reports **4**, 4724 (2014).
 - ²¹ M. Harmand *et al.*, JINST **7**, P08007 (2012).
 - ²² J.-P. Colombier *et al.*, Phys. Rev. B **71**, 165406 (2005).
 - ²³ A. V. Bushman, I. V. Lomonosov, and V. E. Fortov, Sov. Tech. Rev. B Therm. Phys. **5**, 1 (1993).
 - ²⁴ Z. Lin, L. V. Zhigilei, and V. Celli, Phys. Rev. B **77**, 075133 (2008). Mo data are available online on www.faculty.virginia.edu/CompMat/electron-phonon-coupling/
 - ²⁵ F. Deneuville *et al.*, Appl. Phys. Lett. **102**, 194104 (2013).
 - ²⁶ X. Gonze, *et al.*, Comput. Phys. Comm. **180**, 2582 (2009).
 - ²⁷ F. Bottin, S. Leroux, A. Knyazev, G. Zerah, Comput. Mater. Sci. **42**, 329 (2008).
 - ²⁸ J.P. Perdew, K. Burke, M. Ernzerhof, Phys. Rev. Lett. **77**, 3865 (1996).
 - ²⁹ P.E. Blöchl, Phys. Rev. B **41**, 5414 (1990).
 - ³⁰ M. Torrent, F. Jollet, F. Bottin, G. Zerah, Comput. Mater. Sci. **42**, 337 (2008).
 - ³¹ A. Dewaele *et al.*, Phys. Rev. B **78**, 104102 (2008).
 - ³² V. Recoules *et al.* Phys. Rev. B **80**, 64110 (2009).
 - ³³ O. Peyrusse, J. Phys. B **32**, 689 (1999).
 - ³⁴ P. Oelhafen *et al.*, J. Phys.: Condens.Matter **12**, A9 (2000).
 - ³⁵ H. Stupp *et al.*, J. Non-Cryst. Solids **270**, 1 (2000).
 - ³⁶ P. Blaha *et al.* *WIEN2k, An Augmented Plane Wave + Local Orbitals Program for Calculating Crystal Properties*, (Karlheinz Schwarz, Techn. Univ. Wien, Austria, 2001). ISBN 3-9501031-1-2.
 - ³⁷ F. de Groot *et al.*, J. Chem. Phys. **101**, 6570 (1994).
 - ³⁸ Z. Chen *et al.*, Phys. Rev. Lett. **110**, 135001 (2013).
 - ³⁹ P.-M. Leguay *et al.*, Phys. Rev. Lett. **111**, 245004 (2013).
 - ⁴⁰ V. Recoules *et al.* Phys. Rev. Lett. **96**, 055503 (2006).
 - ⁴¹ R. Ernstorfer *et al.*, Science **323**, 1033 (2009).
 - ⁴² E. Bevilion *et al.*, Phys. Rev. B **89**, 115117 (2014).